

Design, Synthesis and Peroxidase-like Activity of 3 α -Helix Proteins Covalently Bound to Heme

Ikuo Obataya,^a Tomoyuki Kotaki,^a Seiji Sakamoto,^a Akihiko Ueno^a and Hisakazu Mihara^{a,b,*}

^aGraduate School of Bioscience and Biotechnology, Tokyo Institute of Technology, Nagatsuta, Yokohama 226-8501, Japan

^bForm and Function, PRESTO, Japan Science and Technology Corporation, Nagatsuta, Midori-ku, Yokohama 226-8501, Japan

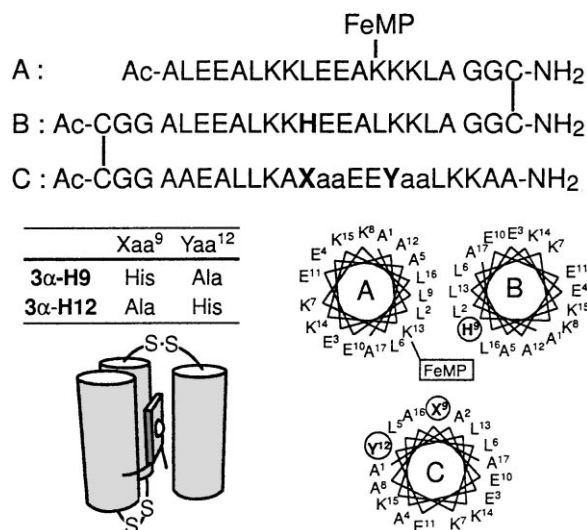
Received 26 July 2000; accepted 23 September 2000

Abstract—As a model of artificial peroxidase, de novo designed three- α -helix proteins, **3 α -H9** and **3 α -H12**, covalently bound to Fe(III)-mesoporphyrin IX were synthesized and examined for a peroxidase-like activity. The activity was regulated according to the positions of His residues in the proteins, and the His residues played a role in an acid–base catalytic function. © 2000 Elsevier Science Ltd. All rights reserved.

Introduction

Peroxidases are hemoproteins that catalyze the oxidation of a large variety of substrates at the expense of hydrogen peroxide.¹ Because of such broad specificity, peroxidases are used as analytical tools or biochemical reagents.² Many attempts have been devoted to obtaining novel molecules bearing the function of peroxidase-like activity.^{3–7} For example, variants of myoglobin have been utilized to compare the structure–activity relationships with peroxidases.³ Although natural hemoproteins can be good candidates to study the function of peroxidases, it is also significantly desired to construct appropriate model proteins with a simplified sequence in a minimal size. So far, many miniaturized hemoproteins have been designed and synthesized, for example, 4 α - or 2 α -helix peptides binding heme non-covalently^{4,5} and 2 α - or $\beta\alpha$ -structures covalently attached to heme.^{6,7} Since these artificial proteins include a heme iron coordinated by two His residues, they are suitable to be applied to a redox function, but not exactly appropriate for the peroxidase-like activity.^{5b} This is because two His residues of natural peroxidases (ex. horseradish peroxidase) are in charge of distinct roles at either the hydrophobic proximal site or the hydrophilic distal site around the porphyrin molecule. The proximal His coordinates to heme iron strongly, whereas the distal His plays roles in deprotonation/protonation of substrates such as hydrogen peroxide involved in the catalytic reaction.⁸ We have attempted to mimic the function of peroxidase by using de novo designed proteins with simple amino acid compositions.⁵ Herein, we have designed 3 α -helix proteins covalently conjugated with heme, focusing on the function of distal His by modulating positions of His residues, in order to regulate 6- or 5-coordination of heme iron (Fig. 1).

nation/protonation of substrates such as hydrogen peroxide involved in the catalytic reaction.⁸ We have attempted to mimic the function of peroxidase by using de novo designed proteins with simple amino acid compositions.⁵ Herein, we have designed 3 α -helix proteins covalently conjugated with heme, focusing on the function of distal His by modulating positions of His residues, in order to regulate 6- or 5-coordination of heme iron (Fig. 1).



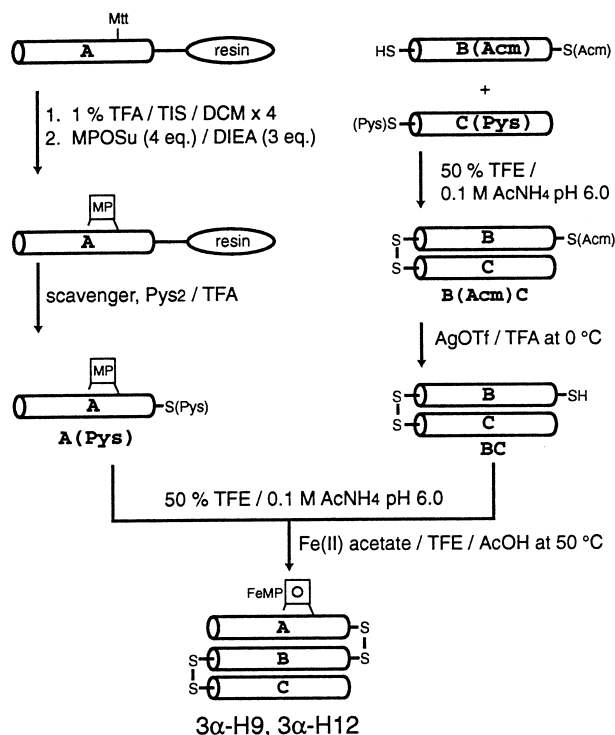
Results and Discussion

The 3 α -helix proteins consist of three amphiphilic helical segments, A, B and C, linked by disulfide bonds of Cys at their N- or C-termini (Fig. 1). Fe(III)-Mesoporphyrin IX (heme) was introduced at the side chain of Lys13 in the segment A to fix the position in the structure. For the design of proximal His residue, a His residue was placed at the 9th position in the hydrophobic region of the segment B. The relative position of HisB9 to LysA13-heme is expected to be favorable for the coordination to heme iron.⁹ In order to control the coordination of the other His to heme iron, the positions of His were varied at 9th and 12th in the segment C for **3 α -H9** and **3 α -H12**, respectively. For **3 α -H9**, two His residues in the segment B and C are expected to bind heme iron in the 6-coordinated form. For **3 α -H12**, only one His residue in the segment B would bind heme iron to form 5-coordination, because His12 in the segment C is apart one turn of α -helix from the optimum position.

The peptide segments were synthesized by using Fmoc-strategy¹⁰ (Scheme 1). Since the segment B(Acm) has two Cys residues for the selective disulfide bonds, one Cys at the C-terminus was protected by the acetamidomethyl (Acm) group. The Cys residue of the segment C was activated with thiopyridine (Pys) by adding 2,2'-dithiodipyridine (Pys₂) at the deprotection step to give C(Pys). The segments B(Acm) and C(Pys) were assembled by stirring in 0.1 M AcNH₄ (pH 6.0) buffer containing 50% trifluoroethanol (TFE) at 25 °C. The resulted assembly of B(Acm)C was purified and lyophilized, and then the Acm group of the segment B was

removed by AgOTf/anisole in trifluoroacetic acid (TFA)¹¹ to obtain the assembly of BC. The peptide resin of the segment A was treated four times with dichloromethane (DCM)/TFA/triisopropylsilane (TIS) (94:1:5) for 2 min to remove the 4-methyltrityl (Mtt) protecting group of Lys13, followed by the coupling with mono-succinimide esterified mesoporphyrin IX (MPOSu). The resin was washed and dried, and then reacted with MPOSu (4 equiv) and *N,N*-diisopropylethylamine (DIEA, 3 equiv) in DCM for 3 h. The mesoporphyrin-conjugated peptide resin was treated with TFA/scavengers with Pys₂ to give the peptide A(Pys). The segment A(Pys) and BC were assembled to a 3 α -helix protein in the buffer. Finally, the iron(III) was inserted into the mesoporphyrin of the protein by mixing with iron(II) acetate in AcOH/TFE (6:4) at 50 °C under nitrogen. The proteins were purified by reversed-phase HPLC (RP-HPLC), and identified by matrix assisted laser desorption time-of-flight MS (MALDI-TOFMS) to give an expected ion peak.¹²

Circular dichroism (CD) measurements of the proteins around the amide region showed typical spectra for an α -helical structure in 20 mM Tris-HCl buffer (pH 7.4) at 25 °C (Fig. 2). The α -helicities were estimated at 70% and 73% for **3 α -H9** and **3 α -H12**, respectively,¹³ suggesting that secondary structures of the proteins were almost identical. UV-vis absorption spectra were measured to investigate environments around Fe(III)-heme or Fe(II)-heme portion of the proteins (Fig. 3). The spectra of reduced Fe(II)-heme were obtained by adding minimum amount of sodium dithionite. The Soret bands of Fe(III)-heme of **3 α -H9** and **3 α -H12** were at 403 nm, which resemble that of bisimidazolyl heme.¹⁴ Visible spectra of Fe(III)-heme of the two proteins were similar to each other with two broad peaks (550 nm and 524 nm) corresponding to the α - and β -bands of the low-spin state heme. However, the Soret band of the reduced Fe(II)-heme implied that the coordination state might be in an equilibrium between 5- and 6-coordination, by displaying a peak at 414 nm with a shoulder at



Scheme 1. Synthesis of 3 α -helix proteins consisting of three peptide segments, A with heme, B and C.

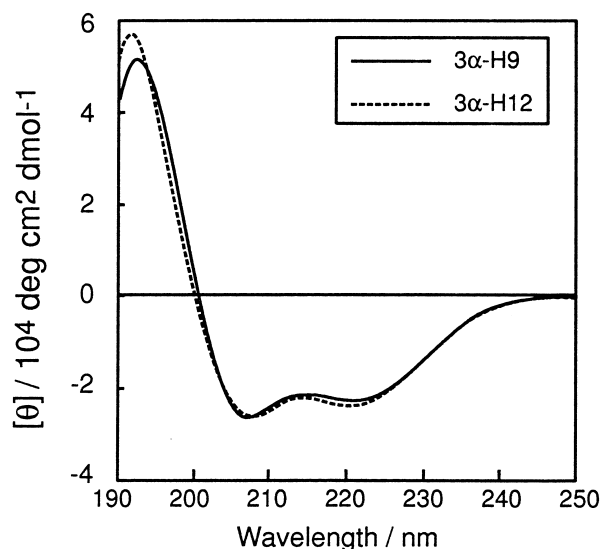


Figure 2. CD spectra at the amide region of the peptides in 20 mM Tris-HCl buffer (pH 7.4) at 25 °C. [**3 α -H9**] = [**3 α -H12**] = 5.0 μ M.

422 nm. These peaks are similar to those corresponding to low-spin (410 nm) or high-spin (417 nm) states of Fe(II)-heme chelated by bis- or mono-imidazole, respectively.¹⁵ The visible spectrum of Fe(II)-heme is sensitive to these coordination states. Six-coordinated (low-spin) Fe(II)-heme shows sharp peaks at the α and β regions, while 5-coordinated (high-spin) Fe(II)-heme, such as that in deoxymyoglobin, has only a broad band around 550 nm.¹³ The spectrum of Fe(II)-heme of **3 α -H9** showed strong signals at α - and β -bands (548 nm and 523 nm), but the peaks lack the sharpness for a typical spectrum of stable 6-coordinated Fe(II)-heme.¹⁴ Therefore, it is likely that the state of **3 α -H9** is predominantly 6-coordination, but includes 5-coordination to some extent. In the case of **3 α -H12**, the spectrum showed two broad peaks without splitting of α/β bands. These results gave the qualitative implication that the 5-coordination state is more abundant in **3 α -H12** than that in **3 α -H9**, which is consistent with our design, particularly, with the arrangement of His residues. It is considered that the equilibrium of the 5/6-coordination can be controlled by modulation of the hydrophobic residues. Since His residues are flanked with Leu residues whose side chains are rotatable in an α -helical structure, **3 α -H9** and **3 α -H12** have fluctuating hydrophobic cores even though they are assembled by two disulfide bonds.

In order to evaluate catalytic activities of the proteins, we investigated steady-state kinetics using formation of tetraguaiacol by oxidation of *o*-methoxyphenol (*o*-MP).¹⁶ The reaction was initiated by adding hydrogen peroxide in 100 mM Tris–HCl buffer (pH 7.4) at 25 °C monitoring absorbance of the product at 470 nm ($\epsilon = 26600$). With excess amounts of a substrate (*o*-MP), the reaction with hydrogen peroxide was the rate-limiting step. Initial rates (v_0) at various concentrations of hydrogen peroxide were plotted to give saturation curves. These curves were fitted using the Michaelis–Menten equation.

$$v_0 = \frac{k_{\text{cat}}[E]_{\text{T}}}{1 + K_{\text{m}}/[H_2O_2]},$$

where $[E]_{\text{T}}$ is total concentration of the catalyst. Obtained kinetic parameters provided clear differences among **3 α -H9**, **3 α -H12** and Fe(III)-mesoporphyrin IX (**FeMP**) (Table 1). The K_{m} values of the catalysts were in the order **3 α -H12** < **FeMP** < **3 α -H9**, suggesting that **3 α -H9** with the 6-coordinated heme inhibited access of hydrogen peroxide. As Sakamoto et al. demonstrated,^{5b} the peroxidase-like function is significantly suppressed by the formation of stable 6-coordinated heme. In contrast, hydrogen peroxide was more efficiently accessible to **3 α -H12** than others, because its heme iron seems not to be fully occupied unlike that in **3 α -H9**. The k_{cat} values of the catalysts were in the order **3 α -H9** > **3 α -H12** > **FeMP**. Under the conditions of large amounts of hydrogen peroxide, it is proposed that a porphyrin ring is decomposed at the α -methene bridge by hydroxyl radical homolytically cleaved from hydrogen peroxide.¹⁷ These degradations of heme moiety were observed by UV–vis spectra and HPLC analyses. In the presence of 5.0 mM H_2O_2 without substrate, **3 α -H9** and **3 α -H12** decreased their absorbance of the Soret band at 403 nm to 20% within 5 min, and HPLC also showed the decomposition of the heme moiety. Therefore, k_{cat} is supposed to be influenced by the degradation

Table 1. Kinetic parameters for oxidation reaction of *o*-methoxyphenol using hydrogen peroxide^a

	K_{m} (mM)	k_{cat} (s ^{−1})	$k_{\text{cat}}/K_{\text{m}}$ (M ^{−1} s ^{−1})
3α-H9	4.6	0.38	83
3α-H12	2.7	0.29	110
FeMP	3.5	0.20	57

^a[catalyst] = 5.0 μ M, [*o*-MP] = 10 mM, [H_2O_2] = 0–5.4 mM in 100 mM Tris–HCl buffer (pH 7.4) at 25 °C.

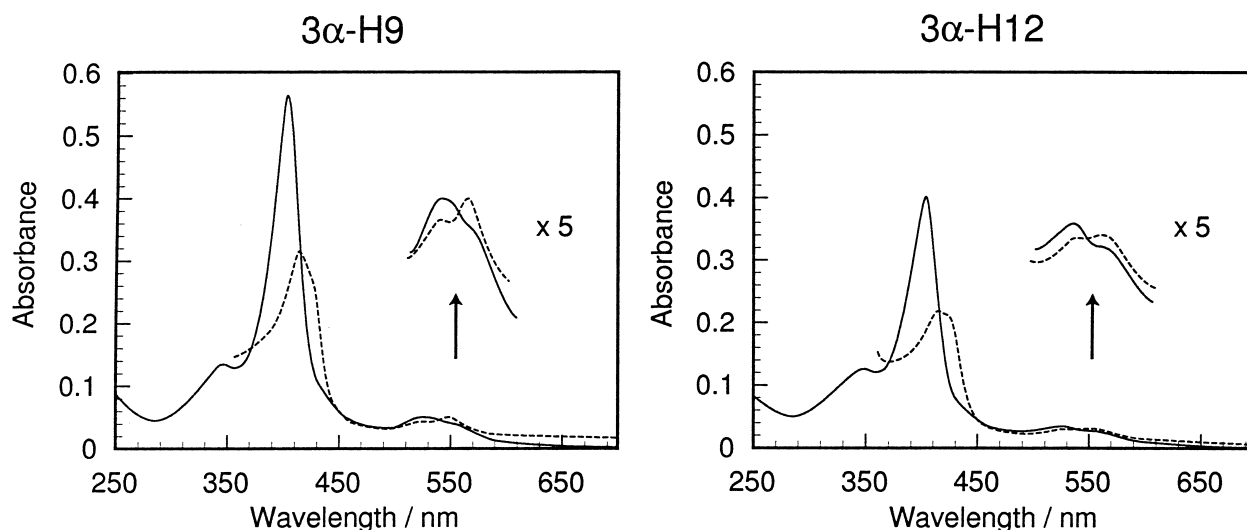


Figure 3. UV–vis spectra of Fe(III)- (solid line) and Fe(II)- (dashed line) mesoporphyrin moiety of the proteins in 20 mM Tris–HCl buffer (pH 7.4) at 25 °C. [**3 α -H9**] = [**3 α -H12**] = 5.0 μ M.

of heme moiety. We suggest that the porphyrin ring of **3 α -H9** is more stable than that of **3 α -H12** and **FeMP** against the radical attack owing to the rigid protection by polypeptide with 6-coordination. Obviously, this protective effect competes against effective incorporation of hydrogen peroxide to heme iron, resulting in the higher K_m of **3 α -H9** discussed above. When the overall function is compared with k_{cat}/K_m values of the proteins, **3 α -H12** shows the highest value, by K_m compensating for the lower k_{cat} than **3 α -H9**.

As shown in Fig. 4, pH profile of the activity ($v_0/[E]_T$) revealed a notable character of **3 α -H12**, displaying a bell-shape curve with maximum activity around pH 7.0. The results proposed that a His residue, probably HisC12, of **3 α -H12** works as an acid–base catalyst as a distal His of natural peroxidases does. The distal His of cytochrome *c* peroxidase has critical roles in the formation of compound I by deprotonation of hydrogen peroxide to form the Fe-OOH intermediate and protonation of OH[−] to release H₂O.⁸ On the other hand, a curve of **3 α -H9** on the pH dependence was similar to **FeMP**, which is not the bell-shape, suggesting that the acid–base catalytic function of **3 α -H9** is weakened compared to that of **3 α -H12**. These results imply that the His residues with stable coordination to heme iron are disadvantageous for the efficient acid–base catalytic function, and also for the access of hydrogen peroxide to heme. These phenomena can be controlled by the design of 3D structure of protein.

In conclusion, we designed and synthesized novel 3 α -helix proteins bearing heme as a peroxidase model. By modulating His positions of the segment C at 9th and 12th, **3 α -H9** and **3 α -H12** were expected to form 6- and 5-coordination, respectively. UV–vis spectra showed that both proteins were in an equilibrium between

6- and 5-coordination and **3 α -H9** included the 6-coordination state more abundantly than **3 α -H12** did. Their catalytic activities correlated with the coordination states of the proteins, as **3 α -H12** displayed a higher activity owing to its small K_m value. The pH profile of the protein activities demonstrated the most significant feature of the acid–base catalytic function of a His residue in **3 α -H12**. It is noteworthy that it is necessary to tune the balance between accessibility of hydrogen peroxide and its destructive effect. **3 α -H12** was successfully designed for the function of distal His, but it was also liable to be decomposed by hydrogen peroxide. Natural peroxidases have evolved to have the ability to cleave the O–O bond of hydrogen peroxide heterolytically by a ‘push–pull effect’ without producing toxic hydroxyl radical.¹ Further tuning of this 3 α -helix scaffold will improve its function by modulating residues around heme and two His residues.

References and Notes

- (a) Dunford, H. B. In *Peroxidases in Chemistry and Biology*; Everse, J., Everse, K. E., Grisham, M. B., Eds.; CRC: Boca Raton, 1991; Vol. 2, pp 1–24. (b) Banci, L. *J. Biotech.* **1997**, *53*, 253.
- van Deurzen, M. P. J.; van Rantwijk, F.; Sheldon, R. A. *Tetrahedron* **1997**, *53*, 13183.
- Grisham, M. B.; Everse, J. In *Peroxidases in Chemistry and Biology*; Everse, J., Everse, K. E., Grisham, M. B., Eds.; CRC Press: Boca Raton, 1991; Vol. 2, pp 335–344.
- (a) Choma, C. T.; Lear, J. D.; Nelson, M. J.; Dutton, P. L.; Robertson, D. E.; DeGrado, W. F. *J. Am. Chem. Soc.* **1994**, *116*, 856. (b) Rau, H. K.; DeJonge, N.; Haehnel, W. *Proc. Natl. Acad. Sci. U.S.A.*, **1998**, *95*, 11526. (c) Arnold, P. A.; Shelton, W. R.; Benson, D. R. *J. Am. Chem. Soc.* **1997**, *119*, 3181.
- (a) Sakamoto, S.; Ueno, A.; Mihara, H. *Chem. Commun.* **1998**, 1073. (b) Sakamoto, S.; Obataya, I.; Ueno, A.; Mihara, H. *J. Chem. Soc., Perkin Trans. 2* **1999**, 2059.
- (a) Natri, F.; Lombardi, A.; Morelli, G.; Maglio, O.; D'Auria, G.; Pedone, C.; Pavone, V. *Chem. Eur. J.* **1997**, *3*, 340. (b) Benson, D. R.; Hart, B. R.; Zhu, X.; Doughty, M. B. *J. Am. Chem. Soc.* **1995**, *117*, 8502.
- Tomizaki, K.-Y.; Nishino, H.; Kato, T.; Miike, A.; Nishino, N. *Chem. Lett.* **2000**, 648.
- Erman, J. E.; Vitello, L. B.; Miller, M. A.; Shaw, A.; Brown, A. K.; Kraut, J. *Biochemistry* **1993**, *32*, 9798.
- Arnold, P. A.; Benson, D. R.; Brink, D. J.; Hendrich, M. P.; Jas, G. S.; Kennedy, M. L.; Petasis, D. T.; Wang, M. *Inorg. Chem.* **1997**, *36*, 5306.
- Chan, W. C.; White, P. D. In *Fmoc Solid Phase Peptide Synthesis: A Practical Approach*; Chan, W. C., White, P. D., Eds.; Oxford University Press: New York, 2000; pp 41–76.
- Fujii, N.; Otaka, A.; Watanabe, T.; Okamachi, A.; Tamamura, H.; Yajima, H.; Inagaki, Y.; Nomizu, M.; Asano, K. *Chem. Commun.* **1989**, 283.
- 3 α -H9** m/z 7213.4 ($[M+Na]^+$ calcd 7213.2); **3 α -H12** m/z 7191.9 ($[M+H]^+$ calcd 7191.2).
- Scholtz, J. M.; Qian, H.; York, E. J.; Stewart, J. M.; Baldwin, R. L. *Biopolymers* **1991**, *31*, 1463.
- Adar, F. In *The Porphyrins*; Dolphin, D., Eds.; Academic: New York, 1979; Vol. 3, pp 167–270.
- Traylor, T. G.; Chang, C. K.; Geibel, J.; Berzinis, A.; Mincey, T.; Cannon, J. *J. Am. Chem. Soc.* **1979**, *101*, 6716.
- Fujita, A.; Senzu, H.; Kunitake, T.; Hamachi, I. *Chem. Lett.* **1994**, 1219.
- Florence, T. M. *J. Inorg. Biochem.* **1985**, *2*, 131.

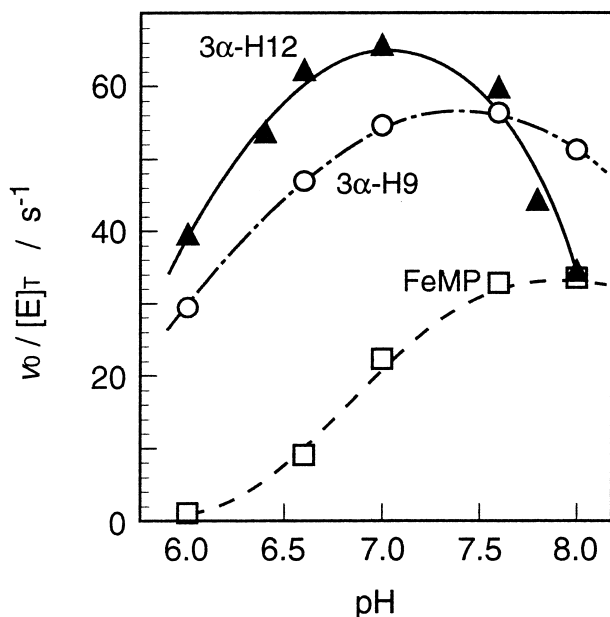


Figure 4. $v_0/[E]_T$ versus pH profiles of **3 α -H9** (circle), **3 α -H12** (triangle) and **FeMP** (square). [**3 α -H9**] = [**3 α -H12**] = 4.4 μ M, [**FeMP**] = 4.4 μ M with 10 μ M of imidazole, [o-MP] = 10 mM, [H₂O₂] = 0.5 mM in 50 mM phosphate buffer at 25 °C.